

# Quasiclassical description of transport through superconducting contacts

J. C. Cuevas

*Institut für Theoretische Festkörperphysik, Universität Karlsruhe, D-76128 Karlsruhe, Germany*

M. Fogelström

*Institute of Theoretical Physics, Chalmers University of Technology and Göteborgs University, S-41296 Göteborg, Sweden  
and Institut für Theoretische Festkörperphysik, Universität Karlsruhe, D-76128 Karlsruhe, Germany*

(Received 19 December 2000; revised manuscript received 6 April 2001; published 2 August 2001)

We present a formulation of boundary conditions that mimics interfaces for the quasiclassical theory of superconductivity and that are suitable for the analysis of transport properties of a great variety of superconducting contacts. These boundary conditions are based on a description of an interface in terms of a simple Hamiltonian. We show how this Hamiltonian description is incorporated into quasiclassical theory via a  $T$ -matrix equation by integrating out irrelevant energy scales right at the onset. The resulting boundary conditions are then explicitly shown to reproduce results obtained by conventional quasiclassical boundary conditions, or by boundary conditions based on the scattering approach. The presented formalism is well suited for the analysis of magnetically active interfaces as well as for calculating time-dependent properties such as the current-voltage characteristics or as current fluctuations in junctions with arbitrary transmission and bias voltage. As a particular implementation of the boundary conditions, we discuss the use of shot noise for the measurement of charge transferred in a multiple Andreev reflection in  $d$ -wave superconductors.

DOI: 10.1103/PhysRevB.64.104502

PACS number(s): 74.50.+r, 74.25.Ha, 74.80.Fp

## I. INTRODUCTION

Electron transport through superconducting junctions is one of the more powerful tools to study properties of the superconducting state in a material. For instance, using quasiparticle tunneling one may directly probe the spectroscopic energy gap induced by the pairing of electrons<sup>1</sup> or by looking at the Josephson effects, dc and ac, the macroscopic phase coherence of the superconducting state may be explored.<sup>2</sup> Methods of electron transport have successfully been carried on to study novel properties of unconventional superconductors such as the heavy fermion systems,<sup>3–5</sup> the high- $T_c$  cuprates,<sup>6–9</sup> and, lately,  $\text{Sr}_2\text{RuO}_4$ .<sup>10–12</sup> Here the phase sensitivity of this class of probes has been used to map out the orbital dependence, i.e., the momentum dependence, of the magnitude and the phase of the superconducting order parameter.<sup>6,7,9</sup> Moving over to the field of mesoscopic superconductivity, electronic transport through various hybrid structures has been used to study the effects of proximity induced superconductivity.<sup>13–15</sup> As an example, the ac Josephson effect has been used to resolve individual conduction channels in single-atom contacts.<sup>16</sup> Finally, combining superconducting and magnetic materials a different class of phenomena is emerging from the competition of two ordered but usually mutually exclusive states of matter.<sup>17–22</sup> Most notable are perhaps the recent experiments showing that the Josephson coupling of two superconductors can be tuned by the magnetic properties of the material making up the barrier separating the two.

In common for the apparently diverse set of experiments above is that a large part in the success of extracting detailed information from measurements is due to the theoretical understanding of electron transport through superconducting contacts. But not only is the correct description of the contact in itself crucial. Also the superconducting state in the vicinity

of the barrier may be significantly different from the bulk superconducting state and must be properly accounted for. This is done by introducing boundary conditions accounting for hard surfaces and barriers of variable transparency into the quasiclassical theory of superconductivity.<sup>23</sup> This theory provides a full description of superconducting phenomena ranging from inhomogeneous superconductors to superconducting phenomena far from equilibrium in the limit of weak perturbations. Weak in the sense that the external perturbations (magnetic field, variations in the chemical potential, etc.) should be small compared to the Fermi energy  $E_F$  of a long wavelength ( $q \gg \lambda_F$ ) compared to the Fermi wavelength  $\lambda_F$  and of low frequency ( $\hbar \omega \ll E_F$ ).<sup>24</sup> Interfaces and surfaces are strong perturbations on the quasiclassical scale and must be incorporated into the quasiclassical theory by effective boundary conditions. These are the so-called Zaitsev boundary conditions<sup>25</sup> with the generalization to magnetically active interfaces by Millis, Rainer, and Sauls.<sup>26</sup> The boundary conditions provide a formal solution to the problem of a strong perturbation due to interfaces but their highly nonlinear form is problematic to handle, e.g., these boundary conditions have spurious solutions which require special care, in particular in numerical implementations. In a recent set of papers<sup>27–29</sup> the Zaitsev-Millis-Rainer-Sauls boundary conditions have been explicitly solved by projecting out these spurious solutions. This is achieved using the powerful Riccati reparametrization of the quasiclassical propagators.<sup>30,31,27</sup>

In this paper we go back a step and generalize the Zaitsev-Millis-Rainer-Sauls boundary conditions to include a wider range of contact types using a Hamiltonian approach.<sup>32–35</sup> In this approach the contact is viewed as a strong local perturbation or as a strong impurity site rather than as a scattering problem and as such it is incorporated into the theory via the conventional many-body perturbation

theory. As it turns out, and this we show explicitly, the resulting boundary conditions arrived at reproduce the results of the Zaitsev-Millis-Rainer-Sauls boundary conditions in the limit of conserved momentum parallel to the interface. On the other hand, the new boundary conditions are more general in the sense that the coupling element across the interface is a free parameter constrained only by symmetry. This allows us to describe disordered junctions or junctions where several momentum directions interfere in the transport across the interfaces. Another advantage of the presented boundary conditions, which we demonstrate by calculation, is their relative simplicity in describing time-dependent phenomena such as the current-voltage characteristics and the current noise spectra of  $S$ - $I$ - $S$  junctions. Finally, the boundary conditions are stable for numerical computations as they do not generate spurious solutions. They are also readily used together with the effective Riccati parametrization of the quasiclassical propagators.

The paper is organized in the following manner: In Sec. II we give the energy integration of the Hamiltonian approach and state the resulting boundary conditions. In Sec. III we show how the current through a contact may be calculated from the boundary  $T$  matrix. In this section we also calculate the Josephson current resolved in energy and on trajectory for different types of superconductors and for different types of coupling between the two superconductors. In Sec. IV, we discuss the boundary conditions at a finite bias applied between two superconductors. This is then applied to the case of two coupled  $d$ -wave superconductors. Finally, in Sec. V, we apply the theory to calculate current fluctuations of two coupled  $d$ -wave superconductors.

## II. DESCRIPTION OF THE APPROACH

The system of study is two semi-infinite superconducting electrodes coupled over some type of interface barrier. Our approach is to artificially separate the problem into two parts in order to pose a boundary condition for the interface. The first part consists of calculating the Green's function of either conductor, extending to  $\pm\infty$ , respectively, in the presence of a hard surface at  $x=0$ . For this part of the problem, the quasiclassical theory<sup>23</sup> is our theory of choice. It has been shown that strong perturbations, such as rigid walls, may be included into quasiclassical theory by means of effective boundary conditions posed for the quasiclassical Green's function.<sup>36,24,37</sup> To couple the two electrodes, from now denoted left ( $L$ ) and right ( $R$ ), we assume a phenomenological Hamiltonian as follows:<sup>34,35</sup>

$$\hat{H}_T = \sum_{\sigma} \hat{c}_{L,\sigma}^{\dagger} v_{LR} \hat{c}_{R\sigma} + \hat{c}_{R\sigma}^{\dagger} v_{RL} \hat{c}_{L\sigma}. \quad (1)$$

The potentials  $v_{LR}$  and  $v_{RL}$ , with  $v_{RL}^{\dagger} = v_{LR} = v$ , act as hopping elements connecting the two electrodes  $L$  and  $R$ . As we explain in detail below, the coupling  $v$  may contain internal quantum numbers, like momentum or spin, which permit the modeling of different types of interfaces. The perturbation given by  $\hat{H}_T$  is short ranged ( $\sim \lambda_F \ll \xi_0$ ) and may be strong ( $v \sim E_F$ ). The local character of  $\hat{H}_T$  allows us to view it as a

single strong impurity in the case of a point contact or as a line of strong impurities in the case of an extended contact between the two electrodes. Following the work of Thuneberg and co-workers<sup>38,39</sup> the single impurity or, in the case of the line of impurities following the work of Buchholtz and Rainer,<sup>36</sup> this strong perturbation may also be incorporated into quasiclassical theory via a  $T$ -matrix equation. Anticipating the result for the  $T$  matrix, the effect of the contact between the two electrodes on the physical quasiclassical Keldysh-Nambu matrix Green's function, or propagator  $\check{g}_i$ , in electrode  $i=(L,R)$  enters as a source term in the transport equation for  $\check{g}_i(\hat{\mathbf{p}}_F)$  along a trajectory  $\hat{\mathbf{p}}_F$ ,

$$i\mathbf{v}_F \cdot \nabla_R \check{g}_i(\hat{\mathbf{p}}_F) + [\check{\epsilon}_i(\hat{\mathbf{p}}_F) - \check{\Delta}_i(\hat{\mathbf{p}}_F), \check{g}_i(\hat{\mathbf{p}}_F)]_{\otimes} = [\check{t}_{ii}(\hat{\mathbf{p}}_F, \hat{\mathbf{p}}_F), \check{g}_{\infty,i}(\hat{\mathbf{p}}_F)]_{\otimes} \delta(\mathbf{R} - \mathbf{R}_c). \quad (2)$$

Here  $\mathbf{R}_c$  is the position of the contact and  $\mathbf{v}_F$  is the Fermi velocity at point  $\hat{\mathbf{p}}_F$  on the Fermi surface. The Green's function  $\check{g}_{\infty,i}$  is an intermediate Green's function obtained by solving the hard wall boundary condition of the separate electrodes, i.e., without taking the contact into account but using the self-energies  $\check{\epsilon}_i$  and  $\check{\Delta}_i$  evaluated using the physical propagator  $\check{g}_i$ , satisfying Eq. (2).

Our objective is to find the quasiclassical  $T$  matrix  $\check{t}$ , giving the source term in the transport Eq. (2) above. The starting point is a conventional many-body perturbation theory for the Hamiltonian  $\hat{H}_T$ . To proceed we artificially enlarge our Hilbert space with a "reservoir quantum number" ( $L,R$ ) and the functions entering are the matrices

$$\begin{aligned} \tilde{\check{G}} &= \begin{pmatrix} \check{G}_{LL} & \check{G}_{LR} \\ \check{G}_{RL} & \check{G}_{RR} \end{pmatrix} & \tilde{\check{T}} &= \begin{pmatrix} \check{T}_{LL} & \check{T}_{LR} \\ \check{T}_{RL} & \check{T}_{RR} \end{pmatrix}, \\ \tilde{\check{G}}_{\infty} &= \begin{pmatrix} \check{G}_{\infty,L} & 0 \\ 0 & \check{G}_{\infty,R} \end{pmatrix} & \tilde{\check{v}} &= \begin{pmatrix} 0 & \check{v}_{LR} \\ \check{v}_{RL} & 0 \end{pmatrix}. \end{aligned}$$

The matrix elements are the usual Keldysh-Nambu matrices of nonequilibrium superconductivity.<sup>24</sup> Especially, the Green's functions  $\check{G}_{\infty,L}$  and  $\check{G}_{\infty,R}$  are the Green's functions for the uncoupled left and right electrode. The coupling elements  $\check{v}_{LR,RL}$  between  $L$  and  $R$  are proportional to the unit matrix in the Keldysh space and in Nambu space adopt the form

$$\hat{v}_{LR} = \hat{v}_{RL}^{\dagger} = \begin{pmatrix} v & 0 \\ 0 & -v^{\dagger} \end{pmatrix}.$$

With this, we write the  $T$ -matrix equation

$$\tilde{\check{T}} = \tilde{\check{v}} + \tilde{\check{v}} \circ \tilde{\check{G}}_{\infty} \circ \tilde{\check{T}} \quad (3)$$

$$= \tilde{\check{v}} + \tilde{\check{v}} \circ \tilde{\check{G}} \circ \tilde{\check{v}}, \quad (4)$$

which together with the Dyson equation

$$\tilde{G} = \tilde{G}_\infty + \tilde{G}_\infty \circ \tilde{T} \circ \tilde{G}_\infty \quad (5)$$

$$= \tilde{G}_\infty + \tilde{G}_\infty \circ \tilde{v} \circ \tilde{G} \quad (6)$$

constitutes a closed set of equations that are to be brought into quasiclassical form. We have given two different ways of summing the series which correspond either to ‘‘dressing’’ the perturbation [Eqs. (3) and (5)] or to dressing the Green’s function [Eqs. (4) and (6)]. The two sets of equations are equivalent and two useful relations,

$$\tilde{v} \circ \tilde{G} = \tilde{T} \circ \tilde{G}_\infty \quad \text{and} \quad \tilde{G}_\infty \circ \tilde{T} = \tilde{G} \circ \tilde{v}, \quad (7)$$

follow directly. Here, and above, the  $\circ$  product is shorthand for integration or summation over common arguments. Starting from Eq. (4), using Eq. (6) and the second of the two relations (7), it is straightforward to get the following closed set of equations, closed separately for one and each of the components  $\check{T}_{ij}$  of the  $T$  matrix:<sup>35</sup>

$$\begin{aligned} \check{T}_{LL} &= \check{v}_{LR} \circ \check{G}_{\infty,R} \circ \check{v}_{RL} + \check{v}_{LR} \circ \check{G}_{\infty,R} \circ \check{v}_{RL} \circ \check{G}_{\infty,L} \circ \check{T}_{LL}, \\ \check{T}_{RR} &= \check{v}_{RL} \circ \check{G}_{\infty,L} \circ \check{v}_{LR} + \check{v}_{RL} \circ \check{G}_{\infty,L} \circ \check{v}_{LR} \circ \check{G}_{\infty,R} \circ \check{T}_{RR}, \\ \check{T}_{LR} &= \check{v}_{LR} + \check{v}_{LR} \circ \check{G}_{\infty,R} \circ \check{v}_{RL} \circ \check{G}_{\infty,L} \circ \check{T}_{LR}, \\ \check{T}_{RL} &= \check{v}_{RL} + \check{v}_{RL} \circ \check{G}_{\infty,L} \circ \check{v}_{LR} \circ \check{G}_{\infty,R} \circ \check{T}_{RL}. \end{aligned} \quad (8)$$

The equations above depend only on the Green’s functions  $\check{G}_{\infty,L}$  and  $\check{G}_{\infty,R}$  of the two uncoupled systems. Since the full Green’s function  $\check{G}_{ij}$  has been eliminated from the  $T$ -matrix equations there are no Green’s functions with spatial arguments in both systems. Together with the short range of  $\check{v}_{LR,RL}$  this means that we can directly perform the quasiclassical  $\xi$  integration on the  $T$ -matrix equations and substitute the quasiclassical Green’s functions  $\check{g}_{\infty,i}$  for the full ones  $\check{G}_{\infty,i}$ , above. As usual the quasiclassical propagator is defined as follows:<sup>24</sup>

$$\check{g}_{\infty,i}(\hat{\mathbf{p}}_F, t, t') = \frac{1}{\pi N_F} \int d\xi \check{\tau}_3 \check{G}_{\infty,i}(\mathbf{p}, t, t'),$$

where  $\xi = v_F(p - p_F)$  and  $N_F$  is the density of states at the Fermi level in the normal state. Notice that, as defined above, the quasiclassical propagators fulfill the normalization condition  $\check{g}_{\infty,i}^2 = -\pi^2$ . In the same way, after the quasiclassical integration of the  $T$ -matrix equation we can replace  $\check{v}$  and  $\check{T}$  by their Fermi surface limits  $\check{v}$  and  $\check{t}$ ,

$$\check{v}_{ij}(\hat{\mathbf{p}}_F, \hat{\mathbf{p}}'_F) = \pi N_F \check{v}_{ij}(\mathbf{p}, \mathbf{p}') \check{\tau}_3,$$

$$\check{t}_{ij}(\hat{\mathbf{p}}_F, \hat{\mathbf{p}}'_F, t, t') = \pi N_F \check{t}_{ij}(\mathbf{p}, \mathbf{p}', t, t') \check{\tau}_3.$$

At the quasiclassical level, the Green’s functions  $\check{g}_{\infty,i}(\hat{\mathbf{p}}_F; t, t')$  at the interface in Eqs. (8) depend on the position on the Fermi surface  $\hat{\mathbf{p}}_F$  and of two times  $(t, t')$ . The coupling elements will be assumed to be time independent

but may couple different points  $\hat{\mathbf{p}}_F$  and  $\hat{\mathbf{p}}'_F$  on the Fermi surfaces of the two conductors. The exact form of the  $(\hat{\mathbf{p}}_F, \hat{\mathbf{p}}'_F)$  dependence of  $\check{v}_{LR}$  is a degree of freedom in the model that allows us to consider different types of transport through the interface. We can now write down the equations for the quasiclassical  $\check{t}$ -matrix components:

$$\begin{aligned} \check{t}_{LL} &= \langle \check{v}_{LR} \otimes \check{g}_{\infty,R} \otimes \check{v}_{RL} \rangle_{\hat{\mathbf{p}}_F}'' \\ &+ \langle \langle \check{v}_{LR} \otimes \check{g}_{\infty,R} \otimes \check{v}_{RL} \otimes \check{g}_{\infty,L} \otimes \check{t}_{LL} \rangle_{\hat{\mathbf{p}}_F}'' \rangle_{\hat{\mathbf{p}}_F}''', \\ \check{t}_{RR} &= \langle \check{v}_{RL} \otimes \check{g}_{\infty,L} \otimes \check{v}_{LR} \rangle_{\hat{\mathbf{p}}_F}'' \\ &+ \langle \langle \check{v}_{RL} \otimes \check{g}_{\infty,L} \otimes \check{v}_{LR} \otimes \check{g}_{\infty,R} \otimes \check{t}_{RR} \rangle_{\hat{\mathbf{p}}_F}'' \rangle_{\hat{\mathbf{p}}_F}''', \\ \check{t}_{LR} &= \check{v}_{LR} + \langle \langle \check{v}_{LR} \otimes \check{g}_{\infty,R} \otimes \check{v}_{RL} \otimes \check{g}_{\infty,L} \otimes \check{t}_{LR} \rangle_{\hat{\mathbf{p}}_F}'' \rangle_{\hat{\mathbf{p}}_F}''', \\ \check{t}_{RL} &= \check{v}_{RL} + \langle \langle \check{v}_{RL} \otimes \check{g}_{\infty,L} \otimes \check{v}_{LR} \otimes \check{g}_{\infty,R} \otimes \check{t}_{RL} \rangle_{\hat{\mathbf{p}}_F}'' \rangle_{\hat{\mathbf{p}}_F}''', \end{aligned} \quad (9)$$

where we suppressed the explicit dependence of the functions on  $\hat{\mathbf{p}}_F$  and on time variables. The earlier  $\circ$  product in Eq. (8) is replaced by the  $\otimes$  product in the quasiclassical expression. The  $\otimes$  product stands for an integration over a common time variable together with a normal matrix multiplication in the combined Keldysh-Nambu and spin space.<sup>24</sup> A leftover from the  $\xi$  integration is the intermediate averaging over position on the Fermi surface as indicated by  $\langle \cdots \rangle_{\hat{\mathbf{p}}_F} = \int_{FS} \cdots d\hat{\mathbf{p}}_F$ . The quasiclassical  $\check{t}$  matrix entering into Eq. (2) is the forward scattering limit,<sup>39</sup>

$$\check{t}_{ij} = \check{t}_{ij}(\hat{\mathbf{p}}_F, \hat{\mathbf{p}}'_F; t, t'),$$

of Eq. (9) and in general it depends on two times  $(t, t')$ .

Following Ref. 24, let us summarize the procedure for calculating the quasiclassical propagators in the presence of an interface:

(i) To find  $\check{g}_\infty$ , we solve the conventional quasiclassical equations, the Eilenberger equation, or the Usadel equation, for the uncoupled electrodes in equilibrium using hard wall boundary conditions.

(ii) Use  $\check{g}_\infty$  to solve the quasiclassical  $\check{t}$ -matrix Eqs. (9).

(iii) Solve the inhomogeneous quasiclassical Eq. (2) for the physical propagator  $\check{g}$ .

(iv) Use  $\check{g}$  to calculate the ‘‘smooth’’ self-energies  $\check{\epsilon}_i$  and  $\check{\Delta}_i$  which enter the quasiclassical equations for  $\check{g}_\infty$  and for  $\check{g}$ . Finally, all the steps must be repeated until the self-consistency is achieved.

The whole scheme amounts to a set of linear differential equations for  $\check{g}_\infty$  and  $\check{g}$ , coupled in a nonlinear way by the  $\check{t}$ -matrix and the self-energy equations. Substantial simplifications can be achieved in the case of low transmissive tunnel barriers or point contacts. In these cases one can neglect the influence of the neighboring electrodes in the calculation of the self-energies and then the equations for  $\check{g}_\infty$  and  $\check{\epsilon}_i$  and  $\check{\Delta}_i$  decouple.

We end this section by noting that using the Riccati parametrization the procedure above may be simplified considerably. This follows from that in the Riccati scheme one separates the coherence functions into “scattering in” and “scattering out” functions.<sup>27–29</sup> The intermediate surface Green’s functions  $\check{g}_\infty$  may be constructed by scattering in functions alone. To compute the initial values for the scattering out functions we use the physical propagator  $\check{g}$  calculated from the interface  $\check{t}$  matrix. In this way we have the necessary information to construct the physical propagator  $\check{g}$  for every trajectory.

### III. JOSEPHSON CURRENTS

As a first application of the boundary conditions we calculate supercurrent through a variety of contacts connecting two superconducting reservoirs. The analysis of this simple transport property will allow us to illustrate: (i) the calculation of the current in terms of the  $\check{t}$ -matrix components, (ii) the comparison with well-known results, and (iii) the flexibility of this formalism for modeling different types of interfaces.

The current contribution from a given trajectory  $\hat{\boldsymbol{p}}_F$  and at a given energy  $\varepsilon$  may be calculated directly by integrating the transport Eq. (2) along the direction given by  $\boldsymbol{v}_F(\hat{\boldsymbol{p}}_F)$ . This is easily seen as on the considered trajectory away from the contact the physical propagator  $\check{g}_i(\hat{\boldsymbol{p}}_F)$  coincides with the intermediate propagator  $\check{g}_{\infty,i}(\hat{\boldsymbol{p}}_F)$  calculated by the impenetrable surface condition. In absolute vicinity of the contact only the source term in Eq. (2),  $[\check{t}_{ii}(\hat{\boldsymbol{p}}_F, \hat{\boldsymbol{p}}_F), \check{g}_{\infty,i}(\hat{\boldsymbol{p}}_F)]\delta(\boldsymbol{R} - \boldsymbol{R}_c)$ , contributes and results in a jump in the Green’s function. The magnitude of this jump is given by integrating Eq. (2) over the interval  $]0_-, 0_+[$ . Performing the integral results in the scattered propagator

$$\check{g}_{i+}(\hat{\boldsymbol{p}}_F) = \check{g}_{i-}(\hat{\boldsymbol{p}}_F) - \frac{i}{v_F \cos \phi_i} [\check{t}_{ii}(\hat{\boldsymbol{p}}_F, \hat{\boldsymbol{p}}_F), \check{g}_{i-}(\hat{\boldsymbol{p}}_F)], \quad (10)$$

where  $\phi_i$  is the angle  $\boldsymbol{v}_F(\hat{\boldsymbol{p}}_F)$  makes with the contact normal. Note that  $\check{g}_{i-}(\hat{\boldsymbol{p}}_F) \equiv \check{g}_{\infty,i}(\hat{\boldsymbol{p}}_F)$  and to calculate  $\check{g}_{i+}(\hat{\boldsymbol{p}}_F)$ , i.e., the propagator along the trajectory ( $\hat{\boldsymbol{p}}'_F$ ) coupled to ( $\hat{\boldsymbol{p}}_F$ ) by pure surface scattering we must solve for  $\check{g}_{i+}(\hat{\boldsymbol{p}}'_F)$  along the path given by  $\boldsymbol{v}_F(\hat{\boldsymbol{p}}'_F)$ . The propagator at the contact, computed in Eq. (10), may now be inserted in the current formula

$$\begin{aligned} j(T) &= eN_F \int \frac{d\varepsilon}{4\pi i} \text{Tr}(\boldsymbol{v}_F(\hat{\boldsymbol{p}}_F) g^K(\hat{\boldsymbol{p}}_F; \varepsilon))_{\hat{\boldsymbol{p}}_F} \\ &= eN_F \int \frac{d\varepsilon}{4\pi i} \langle j_\varepsilon^K(\hat{\boldsymbol{p}}_F) \rangle_{\hat{\boldsymbol{p}}_F}, \end{aligned} \quad (11)$$

with  $N_F$  the density of states at the Fermi level in the normal state. Since the Josephson current is an equilibrium property, the Keldysh Green’s-function components of  $\check{g}$  are in this case simply related to the retarded (R) and advanced (A) ones as  $\hat{g}^K = (\hat{g}^R - \hat{g}^A) \tanh(\varepsilon/2T)$ , and with  $[\hat{g}^A(\hat{\boldsymbol{p}}_F; \varepsilon)]^\dagger$

$= \hat{\tau}_3 \hat{g}^R(\hat{\boldsymbol{p}}_F; \varepsilon) \hat{\tau}_3$ , we get the energy and trajectory resolved current contribution across the contact, evaluated in the left superconductor, as

$$j_\varepsilon^K(\hat{\boldsymbol{p}}_F) = \text{Im}[\text{Tr}\{i\hat{\tau}_3[\hat{t}_{LL}^R, \hat{g}_{\infty,L}^R]\}] \tanh\left(\frac{\varepsilon}{2T}\right). \quad (12)$$

The lonely first intermediate Green’s function  $\check{g}_{\infty,i}(\hat{\boldsymbol{p}}_F)$  in Eq. (10) explicitly drops out of the current in the angle average since it obeys the impenetrable surface boundary condition.

So far no reference has been made to the modeling of the contact and the  $\hat{t}$ -matrix element  $\hat{t}_{LL}^R$ . The contact model depends on the choice of the momentum dependence of the coupling elements,  $v_{RL}^\dagger = v_{LR} = v(\hat{\boldsymbol{p}}_F, \hat{\boldsymbol{p}}'_F)$ . Two extreme models for the  $(\hat{\boldsymbol{p}}_F, \hat{\boldsymbol{p}}'_F)$  dependence will be considered: a totally disordered contact,  $v(\hat{\boldsymbol{p}}_F, \hat{\boldsymbol{p}}'_F) = v$ , i.e., the coupling across the contact retains no memory of the momentum direction, and a momentum conserving contact with  $v(\hat{\boldsymbol{p}}_F, \hat{\boldsymbol{p}}'_F) = v \delta(\hat{\boldsymbol{p}}_F - \hat{\boldsymbol{p}}'_F)$ . The  $\hat{t}$ -matrix equations for the two types of contact, dropping superfluous indexing, read

$$\hat{t} = \hat{v} \langle \hat{g}_R(\hat{\boldsymbol{p}}_F) \rangle_{\hat{\boldsymbol{p}}_F} \hat{v}^\dagger + \hat{v} \langle \hat{g}_R(\hat{\boldsymbol{p}}_F) \rangle_{\hat{\boldsymbol{p}}_F} \hat{v}^\dagger \langle \hat{g}_L(\hat{\boldsymbol{p}}_F) \rangle_{\hat{\boldsymbol{p}}_F} \hat{t} \quad (13)$$

for the disordered contact and

$$\hat{t}(\hat{\boldsymbol{p}}_F) = \hat{v} \hat{g}_R(\hat{\boldsymbol{p}}_F) \hat{v}^\dagger + \hat{v} \hat{g}_R(\hat{\boldsymbol{p}}_F) \hat{v}^\dagger \hat{g}_L(\hat{\boldsymbol{p}}_F) \hat{t}(\hat{\boldsymbol{p}}_F) \quad (14)$$

for the momentum conserving contact. For either model, the  $\hat{t}$ -matrix equation above is simple to invert after inserting the retarded Green’s functions  $\hat{g}_R(\hat{\boldsymbol{p}}_F)$  and  $\hat{g}_L(\hat{\boldsymbol{p}}_F)$ ,

$$\hat{g}(\hat{\boldsymbol{p}}_F)_{R(L)} = \begin{pmatrix} g_{R(L)} & f_{R(L)} e^{\pm i\chi/2} \\ -\tilde{f}_{R(L)} e^{\mp i\chi/2} & -g_{R(L)} \end{pmatrix}, \quad (15)$$

with the phase difference  $\chi$  across the junction and the upper (lower) signs of the phase refer to the right (left) electrode. In equilibrium the  $\hat{t}$ -matrix equation is simply an algebraic equation in energy space, which can be trivially inverted. The energy and trajectory resolved current is written

$$\begin{aligned} j_\varepsilon(\hat{\boldsymbol{p}}_F) &= \text{Im} \left( \frac{i\mathcal{D}(f_R \tilde{f}_L e^{i\chi} - f_L \tilde{f}_R e^{-i\chi})}{2 - \mathcal{D} - \mathcal{D} g_R g_L + \frac{\mathcal{D}}{2}(f_R \tilde{f}_L e^{i\chi} + f_L \tilde{f}_R e^{-i\chi})} \right) \\ &\quad \times \tanh\left(\frac{\varepsilon}{2T}\right). \end{aligned} \quad (16)$$

Here we have traded in the coupling strength  $v$  for the transmission coefficient  $\mathcal{D}$ . The two are simply related as<sup>34</sup>

$$\mathcal{D} = \frac{4|v|^2}{(1+|v|^2)^2}. \quad (17)$$

#### A. Josephson current between two $s$ -wave superconductors

Assuming that the two electrodes both are  $s$ -wave superconductors, we have the Green’s functions on either side of the contact,

$$\hat{g}(\hat{\mathbf{p}}_F)_{R(L)} = -\frac{\pi}{\Omega} \begin{pmatrix} \varepsilon & \Delta e^{\pm i\chi/2} \\ -\Delta e^{\mp i\chi/2} & -\varepsilon \end{pmatrix}, \quad (18)$$

where  $\Omega = [\Delta^2 - \varepsilon^2]^{1/2}$ . Since the  $s$ -wave superconductor is isotropic it does not matter which model for the coupling, Eqs. (13) or (14), we choose. Additionally, in the absence of surface depairing effects it is sufficient to know the bulk Green's functions (18) to calculate the current contribution (12). Using Eq. (16) we find the known result that the Josephson current is carried by junction states<sup>40,41</sup> located at  $\varepsilon_J(\chi, T) = \pm \Delta(T)[1 - \mathcal{D} \sin^2(\chi/2)]^{1/2}$ . The total current is the sum of all contributions and reads

$$j(T) = eN_F \mathcal{D} \frac{\pi \Delta(T) \sin \chi}{\left[1 - \mathcal{D} \sin^2 \frac{\chi}{2}\right]^{1/2}} \tanh\left(\frac{\varepsilon_J(\chi, T)}{2T}\right). \quad (19)$$

In Eq. (19) it should be noted that a second temperature dependence enters via the the temperature dependent gap  $\Delta(T)$ .

### B. Josephson current between two $d$ -wave superconductors

To emphasize the modeling of the  $(\hat{\mathbf{p}}_F, \hat{\mathbf{p}}'_F)$  dependence of the coupling across the junction and the importance of using the correct surface Green's functions, we now study the current-phase relation of two  $d$ -wave superconductors. A realization of a  $d$ -wave order parameter is  $\Delta_{\hat{\mathbf{p}}_F} = \Delta \cos 2(\phi_{\hat{\mathbf{p}}_F} - \alpha)$ . The magnitude and sign of  $\Delta_{\hat{\mathbf{p}}_F}$  depends on the position on the Fermi circle and this is measured by the angle  $\phi_{\hat{\mathbf{p}}_F}$  that the angle  $\hat{\mathbf{p}}_F$  makes with the crystal  $\hat{a}$  axis. The angle  $\alpha$  tracks the relative junction-to-crystal  $\hat{a}$ -axis orientation. If  $\alpha = \pm \pi/4$  and specular quasiparticle scattering at the interface is assumed the order parameter seen along a trajectory changes sign at the surface and an Andreev bound state forms at zero energy for every trajectory  $\hat{\mathbf{p}}_F$ .<sup>42</sup> We will stick with the junction realization  $\alpha = \pm \pi/4$ . To incorporate the effect of these surface states into the current-phase relation one must use the surface Green's functions<sup>43,44</sup>

$$\hat{g}(\hat{\mathbf{p}}_F)_{R(L)} = \frac{\pi}{\varepsilon} \begin{pmatrix} \Omega_{\hat{\mathbf{p}}_F} & i s_R \Delta_{\hat{\mathbf{p}}_F} e^{\pm i\chi/2} \\ i s_R \Delta_{\hat{\mathbf{p}}_F} e^{\mp i\chi/2} & -\Omega_{\hat{\mathbf{p}}_F} \end{pmatrix}, \quad (20)$$

where  $\Omega_{\hat{\mathbf{p}}_F} = [\Delta_{\hat{\mathbf{p}}_F}^2 - \varepsilon^2]^{1/2}$ . The factor  $s_R$  discriminates between two types of junction:<sup>43,45</sup>  $s_R = -1$  ( $\alpha_R = \alpha_L$ ) is referred to as a symmetric, and  $s_R = 1$  ( $\alpha_R = -\alpha_L$ ) as a mirror junction. The convention for signs of the phase  $\chi$  are as for the  $s$ -wave superconductor. It should be said before proceeding that we are neglecting the pair-breaking effect of the surface<sup>46</sup> and we assume constant order parameters up to the interface. This is for the sake of simple illustration and for the comparison of analytical results with other boundary conditions.

Turning to the  $\hat{t}$ -matrix equations and starting with the diffusive model of the point contact, one immediately finds that the Josephson current is zero. This follows from the vanishing average,  $\langle \Delta_{\hat{\mathbf{p}}_F} \hat{\mathbf{p}}_F \rangle = 0$ . Due to this property the

anomalous propagators vanish and therefore the Josephson current as well [see Eq. (16)]. In the opposite limit, using the momentum-conserving model (14), the Josephson current is not zero. After inverting the  $\hat{t}$ -matrix equation and evaluating the commutator in Eq. (12), we find the energy resolved current at  $\hat{\mathbf{p}}_F$ ,

$$j_\varepsilon(\hat{\mathbf{p}}_F) = \pm \text{Im} \left[ \mathcal{D} \Delta_{\hat{\mathbf{p}}_F}^2 \left( \frac{\sin \chi}{\varepsilon^2 - \varepsilon_J^2(\chi; \hat{\mathbf{p}}_F)} \right) \right] \tanh\left(\frac{\varepsilon}{2T}\right). \quad (21)$$

The sign of  $j_\varepsilon(\hat{\mathbf{p}}_F)$  is (+) for a mirror and (-) for a symmetric junction. As in the case of the  $s$ -wave junction we have junction states carrying the Josephson current. The position of these states depends on the type of junction in the following way:

$$\varepsilon_J(\chi; \hat{\mathbf{p}}_F) = \pm \sqrt{\mathcal{D}} |\Delta_{\hat{\mathbf{p}}_F}| \begin{cases} \left| \sin \frac{\chi}{2} \right|, & \text{mirror} \\ \left| \cos \frac{\chi}{2} \right|, & \text{symmetric.} \end{cases} \quad (22)$$

These junction states were found by Riedel and Bagwell<sup>47</sup> using a scattering approach and, independently, by Barash<sup>45</sup> using the Zaitsev boundary conditions.<sup>25</sup> Performing the integral over the energy we write the trajectory resolved current-phase relations

$$j(\hat{\mathbf{p}}_F) = \pm 2 \pi \sqrt{\mathcal{D}} |\Delta_{\hat{\mathbf{p}}_F}| \begin{cases} \cos \frac{\chi}{2} \tanh\left(\frac{\sqrt{\mathcal{D}} |\Delta_{\hat{\mathbf{p}}_F}| \sin \frac{\chi}{2}}{2T}\right) \\ \sin \frac{\chi}{2} \tanh\left(\frac{\sqrt{\mathcal{D}} |\Delta_{\hat{\mathbf{p}}_F}| \cos \frac{\chi}{2}}{2T}\right) \end{cases} \quad (23)$$

for the two junction types, the upper being the mirror and the lower the symmetric one. The total current is the trajectory average of  $j(\hat{\mathbf{p}}_F)$  multiplied by  $eN_F$ .

The main purpose of this and the preceding section was to show that the quasiclassical version of the point contact coupling of two electrodes is simple to use and can recover results known in literature. In case of unconventional superconducting electrodes results depend in a crucial way on how the contact is modeled. This gives the Hamiltonian boundary condition an advantage in flexibility to the conventional Zaitsev boundary conditions which coincides with the momentum conserving contact (14) introduced above.

### C. Josephson current through a spin active interface

As another illustration of the flexibility of this method we extend the discussion to currents through spin active interfaces, i.e., interfaces which flip the spin of the incident electrons either by spin-dependent scattering within the interface, or by a difference in spin-orbit coupling on either side of the interface. The general boundary conditions that connect the quasiclassical propagators for superconducting metals across magnetically active interfaces were introduced by Millis,

Rainer, and Sauls.<sup>26</sup> Recently one of the authors<sup>29</sup> derived the explicit solution of these boundary conditions for equilibrium Green functions. In order to compare with this solution, as in Ref. 29, we shall analyze in this section the Josephson current through a contact of two isotropic  $s$ -wave superconductors connected through a small magnetically active junction.

In order to accommodate the spin dependence we enlarge our space in comparison with the two preceding subsections in such a way that every quantity is now a  $2 \times 2$  matrix in spin space. In particular, the coupling elements are spin dependent and may adopt the following general form:

$$\hat{v}_{LR} = \hat{v}_{RL}^\dagger = \begin{pmatrix} v & 0 \\ 0 & v^\dagger \end{pmatrix} \quad \text{where } v = \begin{pmatrix} v_{\uparrow,\uparrow} & v_{\uparrow,\downarrow} \\ v_{\downarrow,\uparrow} & v_{\downarrow,\downarrow} \end{pmatrix}. \quad (24)$$

Let us stick to the case of  $S/F/S$  junction analyzed in Ref. 29. In this case  $F$  stands for a small ferromagnetic particle or grain. This ferromagnetic material is treated as a partially transparent barrier which transmits the two spin projections differently. For spin-active interfaces the different components of the  $S$  matrix,  $S_{ij}$  are  $2 \times 2$  spin matrices. To proceed further a specific  $S$  matrix was chosen in Ref. 29 to model the magnetic barrier

$$\hat{S} = \begin{pmatrix} S_{11} & S_{12} \\ S_{21} & S_{22} \end{pmatrix} = \begin{pmatrix} r & t \\ t & -r \end{pmatrix} \exp(i\Theta \sigma_3), \quad (25)$$

where  $\sigma_j$  notes the Pauli matrices spanning spin space and parameters  $(t, r)$  are the usual transmission and reflection coefficients. The  $S$  matrix (25) is one of the simplest choices that allows a variable degree of spin mixing at the interface and the spin mixing is parametrized by the spin-mixing angle  $\Theta$ . By this construction  $\hat{S}$  only violates spin conservation, i.e., it does not commute with the quasiparticle spin operator  $\sigma$ . The angle  $\Theta$  will be considered as a phenomenological parameter independent of the trajectory direction (for more details see Tokuyasu *et al.*<sup>48</sup>). Within the approach presented in this paper, one can easily model the previous  $S$  matrix with a spin-dependent coupling,

$$\hat{v}_{LR} = \hat{v}_{RL}^\dagger = v \begin{pmatrix} \exp(i\Theta \sigma_3) & 0 \\ 0 & \exp(-i\Theta \sigma_3) \end{pmatrix}. \quad (26)$$

Again the quasiclassical surface Green's functions are the inputs in this approach, i.e., the Green's functions at the interface calculated with impenetrable wall boundary conditions. The spin active boundary conditions must be used at

the contact also for the reflecting surface.<sup>29</sup> In this simple case of a magnetic barrier the resulting spin-dependent propagators can be written in a  $4 \times 4$  block-diagonal form,

$$\hat{g}_{block}(\hat{\mathbf{p}}_F; \Theta) = \begin{pmatrix} \hat{g}(\hat{\mathbf{p}}_F; \Theta) & 0 \\ 0 & \hat{g}(\hat{\mathbf{p}}_F; -\Theta) \end{pmatrix} = \begin{pmatrix} g_{\uparrow\uparrow} & f_{\uparrow\downarrow} & 0 & 0 \\ \tilde{f}_{\downarrow\uparrow} & \tilde{g}_{\downarrow\downarrow} & 0 & 0 \\ 0 & 0 & g_{\downarrow\downarrow} & -f_{\uparrow\downarrow} \\ 0 & 0 & -\tilde{f}_{\downarrow\uparrow} & \tilde{g}_{\uparrow\uparrow} \end{pmatrix}, \quad (27)$$

where the electron and anomalous parts of  $\hat{g}(\hat{\mathbf{p}}_F; \Theta)$  in the upper left corner of  $\hat{g}_{block}(\hat{\mathbf{p}}_F; \Theta)$  can be written as

$$g_{\uparrow\uparrow}(\Theta) = -\pi \frac{\varepsilon^R \cos(\Theta/2) - \Omega \sin(\Theta/2)}{\varepsilon^R \sin(\Theta/2) + \Omega \cos(\Theta/2)}, \quad (28)$$

$$f_{\uparrow\downarrow}(\Theta) = \pi \frac{\Delta e^{-i(\Theta \mp \chi)/2}}{\varepsilon^R \sin(\Theta/2) + \Omega \cos(\Theta/2)},$$

$$\tilde{f}_{\downarrow\uparrow}(\Theta) = -\pi \frac{\Delta e^{i(\Theta \mp \chi)/2}}{\varepsilon^R \sin(\Theta/2) + \Omega \cos(\Theta/2)}$$

for trajectories with  $(\hat{\mathbf{p}}_F \cdot \hat{\mathbf{n}} > 0)$ . For trajectories with reversed momentum, i.e.,  $(\hat{\mathbf{p}}_F \cdot \hat{\mathbf{n}} < 0)$ , the phase factor  $\exp[\mp i(\Theta \mp \chi)/2]$  for functions  $f_{\uparrow\downarrow}(\Theta)$  and  $\tilde{f}_{\downarrow\uparrow}(\Theta)$  goes to  $\exp[\pm i(\Theta \pm \chi)/2]$ . Above, as in the earlier examples, the phase difference  $\chi$  between the two reservoirs is included and the upper (lower) signs refer to the right (left) reservoir. The components of the propagator in the lower right corner of  $\hat{g}_{block}$  are simply related to those in the upper left corner by the replacement  $\Theta \rightarrow -\Theta$ .

The angle  $\Theta$  induces a mixing of the two otherwise separated spin bands. It is easy to see that the resulting density of states at the interface has Andreev bound states inside the gap. These states are located at  $\varepsilon_{b,\uparrow(\downarrow)} = \pm \Delta \cos(\Theta/2)$ , with  $+$  ( $-$ ) for the spin-up ( $-$ down) branch. The existence of the subgap states alters the Josephson current-phase relation radically. The contribution to the current from the energy  $\varepsilon$ , the trajectory  $\hat{\mathbf{p}}_F$ , and spin band  $\uparrow(\downarrow)$  may be calculated directly from expression (16). Keeping in mind that the phase that enters in Eq. (16) is the phase difference over the contact we write

$$j_{\varepsilon,\uparrow}(\hat{\mathbf{p}}_F; \Theta, \chi) = \text{Im} \left[ \mathcal{D} \Delta^2 \left( \frac{\sin \chi}{[\Omega \cos(\Theta/2) + \varepsilon \sin(\Theta/2)]^2 - \mathcal{D} \Delta^2 \sin^2(\chi/2)} \right) \right] \tanh \left( \frac{\varepsilon}{2T} \right) \quad (29)$$

for the current carried by the spin-up band. The current carried by the spin-down band is given simply as  $j_{\varepsilon,\downarrow}(\hat{\mathbf{p}}_F; \Theta, \chi) = j_{\varepsilon,\uparrow}(\hat{\mathbf{p}}_F; -\Theta, \chi)$ . At a finite superconducting

phase difference, the original two interface Andreev bound states are split up into four current carrying states located inside the gap at positions

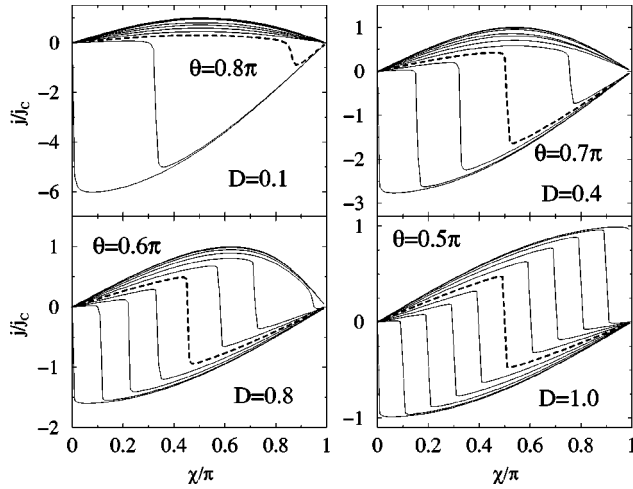


FIG. 1. Zero-temperature supercurrent-phase relation for the  $S/F/S$  contact considered in this section. The four different panels correspond to  $\mathcal{D}=0.1, 0.4, 0.8,$  and  $1.0$ . The spin-mixing angle  $\Theta$  is varied from top to bottom from  $0$  to  $\pi$  in steps of  $\pi/10$ . The dashed lines indicate the first value of  $\Theta$  for which the contacts have become a  $\pi$  junction. The supercurrent is normalized in units of the critical current density  $j_c$  for the corresponding transmission and zero spin-mixing angle.

$$\varepsilon_J = \pm \Delta [\cos^2(\Theta/2) - \mathcal{D} \cos(\Theta) \sin^2(\chi/2) \pm \sqrt{\mathcal{D} \sin(\Theta) \sin(\chi/2) \sqrt{1 - \mathcal{D} \sin^2(\chi/2)}}]^{1/2}. \quad (30)$$

These states give the total contribution to the current and their positions change from the tunnel regime,  $\varepsilon_J = \pm \Delta \cos(\Theta/2)$ , to  $\varepsilon_J = \pm \Delta \cos[(\chi \pm \Theta)/2]$  at perfect transmission. In Fig. 1 we show the current-phase relation for a set of transparencies  $\mathcal{D}=0.1, 0.4, 0.8,$  and  $1.0$ . In each panel the spin-mixing angle  $\Theta$  is varied from  $0$  to  $\pi$  in steps of  $\pi/10$ . As seen, for each value of  $\mathcal{D}$  there is a range  $\Theta > \Theta_c$  where the junctions are  $\pi$  junctions. For small  $\mathcal{D}$ , the critical spin-mixing angle  $\Theta_c$  is close to  $\pi$  and with increasing  $\mathcal{D}$ ,  $\Theta_c$  increases towards  $\pi/2$ . The magnitude of the critical current is for all but the perfect transmission junction very asymmetric for  $0$  and  $\pi$  junctions. In Fig. 2 we show the energy resolved spectral current (29) for  $\mathcal{D}=0.4$  and  $\Theta=0.7\pi$  at different phase differences  $\chi$  over the junction. At small phase differences the junction state initially at  $\varepsilon_J(\chi=0) = \pm \Delta \cos(\Theta/2)$  splits into two states carrying current in opposite directions. This gives a small but positive current as seen in the corresponding current-phase relation in Fig. 1. As the phase difference is increased the two states dispersing with phase towards  $\varepsilon=0$  from either side eventually cross at  $\varepsilon=0$ . Above this phase difference, both current-carrying states at  $\varepsilon < 0$  ( $\varepsilon > 0$ ) give current in the same direction and the magnitude of the current increases abruptly.

To conclude this section, let us stress that these results reproduce the results obtained in Ref. 29, showing again the versatility of the boundary conditions introduced in this work.

#### IV. SOLVING THE $T$ -MATRIX EQUATION AT AN APPLIED VOLTAGE

Probably the main advantage of the present approach lies in the description of time-dependent transport properties like

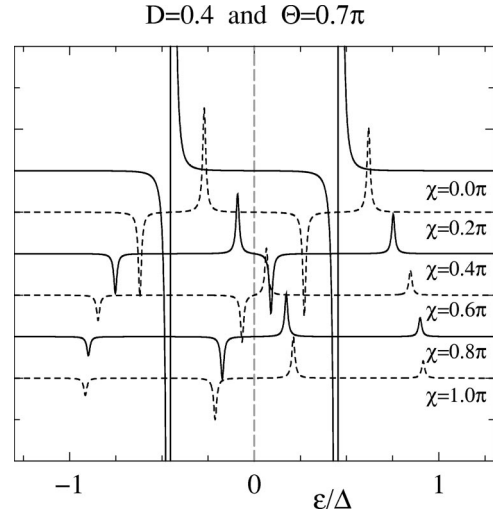


FIG. 2. Energy resolved spectral current for the  $S/F/S$  contact with  $\mathcal{D}=0.4$  and  $\Theta=0.7\pi$  (see Fig. 1, right upper panel). This figure shows the total spectral current, sum of both spin contributions, as a function of energy according to Eq. (29), without the thermal factor. The different curves show the evolution of the four current-carrying Andreev bound states inside the gap with the superconducting phase difference. The curves are shifted vertically for clarity.

current-voltage characteristics and current fluctuations, especially in those situations in which multiple Andreev reflections dominate the electronic transport. In this section we show how the  $\check{t}$ -matrix Eq. (9) can be solved in the case of a voltage-biased superconducting contact. It is worth remarking that the solution described below is rather general and includes unconventional superconductor as well as spin active interfaces. In this sense, this solution constitutes the basis for the analysis of the ac Josephson effect within the quasiclassical theory in many situations which were traditionally out of the scope of this approach.

We shall restrict the discussion to the case of a constant bias voltage. The extension to the case of a time-dependent voltage is rather straightforward. As a constant bias  $V$  is applied across a junction between two superconductors, the phase difference oscillates with the time according to the Josephson relation  $\phi(t) = \phi_0 + \omega_0 t$ , where  $\omega_0 = 2eV/\hbar$  is the Josephson frequency. This means that every Green's function and  $\check{t}$ -matrix component depends on two time arguments. We show in this section how the time convolutions in the  $\check{t}$ -matrix equation can be handled.

As we shall show in the next section the current can be expressed, for instance, only in terms of the advanced and retarded components of  $\check{t}_{LR}$ . Thus we concentrate on those components whose equations can be written as [see Eq. (9)]

$$\hat{t}_{LR}^{R,A}(t,t') = \hat{v}_{LR} + \int dt_1 \int dt_2 \hat{v}_{LR} \hat{g}_R^{R,A}(t,t_1) \times \hat{v}_{RL} \hat{g}_L^{R,A}(t_1,t_2) \hat{t}_{LR}^{R,A}(t_2,t'). \quad (31)$$

Here, we have written explicitly the time convolutions for the sake of clarity and we have omitted the  $\hat{p}_F$  integrations,

since they do not affect the time convolutions. In this expression every quantity is a  $4 \times 4$  matrix in Nambu and spin space, and from now to the end of this section we get rid of the superscripts  $R, A$ , since the equations for these two components are formally identical. We also drop the  $\infty$  subindex, since all propagators in Eq. (31) are propagators of the separated electrodes. The electrode Green's functions entering Eq. (31) take the form  $\hat{g}_j(t, t') = \hat{U}_j^\dagger(t) \hat{g}_j(t-t') \hat{U}_j(t')$ , where  $j=R, L$  and  $\hat{U}_j(t) = \exp[i\phi_j(t)\hat{\tau}_3/2]$ ,  $\phi_j(t)$  being the phase of the  $j$ th superconductor. In this expression,  $\hat{g}_j(t) = \int \hat{g}_j(\epsilon) \exp(-i\epsilon t) d\epsilon/2\pi$ .

We use the transformation generated by  $\hat{U}_j(t)$  to transfer the time dependence from the Green's functions to the hopping elements

$$\hat{t}_{LR}(t, t') = \hat{v}_{LR}(t) \delta(t-t') + \int dt_1 \int dt_2 \hat{v}_{LR}(t) \hat{g}_R(t-t_1) \hat{v}_{RL}(t_1) \hat{g}_L(t_1-t_2) \hat{t}_{LR}(t_2, t'), \quad (32)$$

where  $\hat{v}_{LR}(t) = \hat{U}_L(t) \hat{v}_{LR} \hat{U}_R^\dagger(t) = \hat{v}_{RL}^\dagger(t) = v \exp[i\phi(t)\hat{\tau}_3/2]$ . One can easily show that all physical properties of the system are invariant under this gauge transformation. Thus we shall usually consider the  $\hat{t}$ -matrix equation in this gauge, i.e., in which the hopping elements are time dependent and the electrode Green's functions only depend on the time difference.

In order to solve Eq. (32) it is more convenient to work in energy space where it becomes an algebraic equation. Thus we Fourier transform the  $\hat{t}$  matrix with respect to the temporal arguments

$$\hat{t}_{LR}(t, t') = \frac{1}{2\pi} \int d\epsilon \int d\epsilon' e^{-i\epsilon t} e^{i\epsilon' t'} \hat{t}_{LR}(\epsilon, \epsilon'). \quad (33)$$

It is easy to convince oneself that, due to the special time dependence of the coupling elements, the  $\hat{t}$  matrix admits a Fourier expansion of the form

$$\hat{t}_{LR}(t, t') = \sum_n e^{in\phi(t')/2} \int \frac{d\epsilon}{2\pi} e^{-i\epsilon(t-t')} \hat{t}_{LR}(\epsilon, \epsilon + neV). \quad (34)$$

In other words, Fourier transforming Eq. (32) one can show that  $\hat{t}_{LR}(\epsilon, \epsilon')$  satisfies the following relation:

$$\hat{t}_{LR}(\epsilon, \epsilon') = \sum_n \hat{t}_{LR}(\epsilon, \epsilon + neV) \delta(\epsilon - \epsilon' + neV). \quad (35)$$

As we show below, the problem of the calculation of the current can be reduced to the evaluation of the Fourier components  $\hat{t}_{nm}(\epsilon) \equiv \hat{t}_{LR}(\epsilon + neV, \epsilon + meV)$ . As can be seen by Fourier transforming Eq. (32), these components fulfill the following set of algebraic linear equations:

$$\hat{t}_{nm} = \hat{v}_{nm} \delta_{n, m \pm 1} + \hat{E}_{nm} \hat{t}_{nm} + \hat{V}_{n, n-2} \hat{t}_{n-2, m} + \hat{V}_{n, n+2} \hat{t}_{n+2, m}, \quad (36)$$

where  $\hat{v}_{m-1, m} = v(\hat{1} + \hat{\tau}_3)/2$ ,  $\hat{v}_{m+1, m} = v(\hat{1} - \hat{\tau}_3)/2$ , and the matrix coefficients  $\hat{E}_{nm}$  and  $\hat{V}_{n, m}$  can be expressed in terms of the Green's functions of the uncoupled electrodes, as

$$\begin{aligned} \hat{E}_{nn} &= \begin{pmatrix} v g_{R, n+1} v^\dagger g_{L, n} & v g_{R, n+1} v^\dagger f_{L, n} \\ v^\dagger g_{R, n-1} v \tilde{f}_{L, n} & v^\dagger g_{R, n-1} v g_{L, n} \end{pmatrix}, \\ \hat{V}_{n, n+2} &= -v f_{R, n+1} v \begin{pmatrix} \tilde{f}_{L, n+2} & g_{L, n+2} \\ 0 & 0 \end{pmatrix}, \\ \hat{V}_{n, n-2} &= -v^\dagger \tilde{f}_{R, n-1} v^\dagger \begin{pmatrix} 0 & 0 \\ g_{L, n-2} & f_{L, n-2} \end{pmatrix}. \end{aligned} \quad (37)$$

In these equations the shorthand notation  $g_{i, n} = g_i(\epsilon + neV)$  for the  $2 \times 2$  spin-dependent propagators has been used. Notice that the set of linear Eqs. (36) are analogous to those describing a tight-binding chain with nearest-neighbor hopping parameters  $\hat{V}_{n, n+2}$  and  $\hat{V}_{n, n-2}$ . A solution can then be obtained by standard recursive techniques (see Ref. 35 for details).

Finally, the  $\hat{p}_F$  dependence of the Green's function in Eq. (36) depends on our choice of the contact model. Thus, for instance, for the disordered case, the Green's functions appearing in Eq. (36) are the angle averaged ones, while for the case of a momentum conserving contact we must include the trajectory dependent Green's functions [see Eqs. (13) and (14)].

### Current at finite voltage

As commented in a previous section, the current contribution from a given trajectory may be calculated directly by integrating the transport Eq. (2) along the trajectory over the discontinuity given by the source term. Thus the time-dependent current reads as

$$j(t) = e N_F \langle j(\hat{p}_F, t) \rangle_{\hat{p}_F}, \quad (38)$$

where the contribution of a given trajectory with momentum  $\hat{p}_F$  can be written as

$$j(\hat{p}_F, t) = \text{Tr} \{ \hat{\tau}_3 [ \check{t}_{LL}, \check{g}_{\infty, L} ]_{\otimes}^K \}. \quad (39)$$

This expression can be greatly simplified as follows. First, the Keldysh components of the  $\check{t}$  matrix can be eliminated in favor of the advanced and retarded components using the relation  $\check{t}^K = \check{t}^R \otimes \check{g}_{\infty}^K \otimes \check{t}^A$ . On the other hand, the four elements of the enlarged space are not independent. For instance, it is easy to show the following relations:  $\check{t}_{LR} = (1 + \check{t}_{LL} \otimes \check{g}_{\infty, L}) \otimes \check{v}_{LR}$  and  $\check{t}_{RL} = \check{v}_{RL} \otimes (1 + \check{g}_{\infty, L} \otimes \check{t}_{LL})$ . Using these relations it is rather straightforward to show that the current can be written as<sup>35</sup>

$$\begin{aligned} j(\hat{p}_F, t) &= \text{Tr} [ \hat{\tau}_3 ( \hat{t}_{LR}^R \otimes \hat{g}_R^K \otimes \hat{t}_{RL}^A \otimes \hat{g}_L^A - \hat{g}_L^R \otimes \hat{t}_{LR}^R \otimes \hat{g}_R^K \otimes \hat{t}_{RL}^A \\ &\quad + \hat{g}_R^R \otimes \hat{t}_{RL}^R \otimes \hat{g}_L^K \otimes \hat{t}_{LR}^A - \hat{t}_{RL}^R \otimes \hat{g}_L^K \otimes \hat{t}_{LR}^A \otimes \hat{g}_R^A ) ], \end{aligned} \quad (40)$$

where we have dropped the symbol  $\infty$ , since from now on in this section the only Green functions which will appear are the surface Green functions.

Taking into account the Fourier expansion of the  $\hat{t}$  matrix [see Eq. (34)], the current in a voltage-biased superconducting contact adopts finally the form

$$j(\hat{\mathbf{p}}_F, t) = \sum_{m=-\infty}^{\infty} j_m(\hat{\mathbf{p}}_F) e^{im\phi(t)}, \quad (41)$$

where the different Fourier current components can be expressed in terms of the Fourier components of the harmonics  $\hat{t}_{nm}(\epsilon) \equiv \hat{t}(\epsilon + neV, \epsilon + meV)$  as follows:

$$j_m(\hat{\mathbf{p}}_F) = \int d\epsilon \sum_n \text{Tr} [ \hat{\tau}_3 (\hat{t}_{LR,0n}^R \hat{g}_{R,n}^K \hat{t}_{RL,nm}^A \hat{g}_{L,m}^A - \hat{g}_{L,0}^R \hat{t}_{LR,0n}^R \hat{g}_{R,n}^K \hat{t}_{RL,nm}^A + \hat{g}_{R,0}^R \hat{t}_{RL,0n}^R \hat{g}_{L,n}^K \hat{t}_{LR,nm}^A - \hat{t}_{RL,0n}^R \hat{g}_{L,n}^K \hat{t}_{LR,nm}^A \hat{g}_{R,m}^A ) ]. \quad (42)$$

Finally, one can further simplify the expression of the current harmonics  $j_m$ , making use of the general relation  $\hat{t}_{RL,nm}^{A,R}(\epsilon) = \hat{\tau}_3 \hat{t}_{LR,mn}^{R,A^\dagger}(\epsilon) \hat{\tau}_3$ , which can be deduced from the equations of the  $\hat{t}$ -matrix components. Thus we can express the current just in terms of harmonics  $\hat{t}_{LR,nm}^{R,A}$ , whose calculation was detailed above. Equations (41) and (42) are the basis of the description of the ac Josephson effect in a voltage-biased superconducting contact, covering unconventional superconductors and spin active interfaces.

In order to illustrate our approach in the case of a voltage biased contact, we consider here a junction between two  $d$ -wave superconductors. Let us analyze in particular the symmetric junction mentioned in Sec. III B, whose description is based on the Green's functions of Eq. (20). Again, we neglect pair breaking effects and assume a constant order parameter up to the interface. The proper self-consistent treatment of these junctions will be the subject of a forthcoming publication. In this contact geometry the zero-energy bound states in each side of the interface strongly affect the transport through this system. Of course, the results for the current depend on the contact model used. Let us first consider the case of a disordered contact. In this case, the propagators which enter in the current formula are the angle averaged ones. This implies that the anomalous propagators vanish, which means that the current is only due to single-quasiparticle processes. Thus the current formula reduces to

$$j(V) = eN_F \int_{-\infty}^{\infty} d\epsilon \mathcal{T}(\epsilon, V) [f_{FD}(\epsilon - eV) - f_{FD}(\epsilon)], \quad (43)$$

where  $\mathcal{T}(\epsilon, V)$  is an energy and voltage dependent transmission coefficient given by

$$\mathcal{T}(\epsilon, V) = \frac{4\pi^2 |v|^2 \langle \rho_L(\epsilon - eV) \rangle_{\hat{\mathbf{p}}_F} \langle \rho_R(\epsilon) \rangle_{\hat{\mathbf{p}}_F}}{|1 - |v|^2 \langle g_L(\epsilon - eV) \rangle_{\hat{\mathbf{p}}_F} \langle g_R(\epsilon) \rangle_{\hat{\mathbf{p}}_F}|^2}, \quad (44)$$

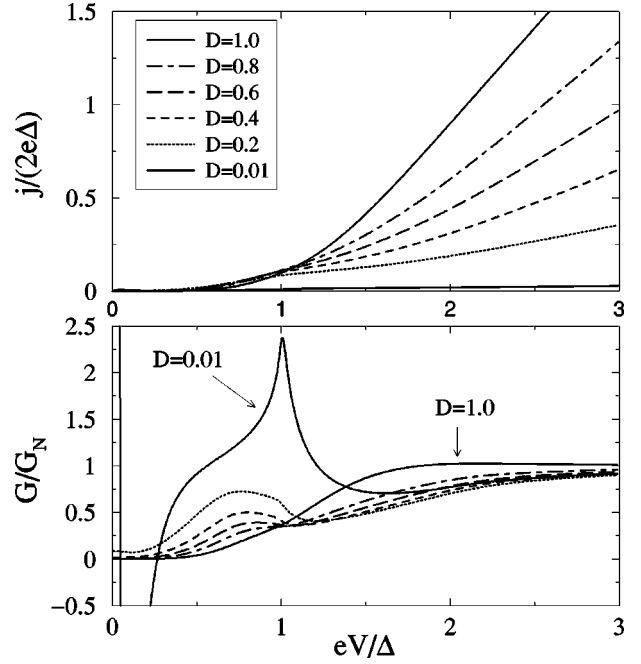


FIG. 3. Zero-temperature  $I$ - $V$  characteristics (upper panel) and differential conductance for different transmissions (lower panel) of a disordered contact between two  $d$ -wave superconductors. The misorientations are  $\alpha = \pi/4$ . The conductance is normalized by the normal-state conductance and the voltage is expressed in units of the maximum gap  $\Delta$ .

where  $\langle \rho_i(\epsilon) \rangle_{\hat{\mathbf{p}}_F}$  ( $i=L,R$ ) is the local density of states at the interface.

In Fig. 3 we show the current-voltage characteristics and differential conductance for different values of the normal transmission coefficient  $\mathcal{D}$  for this disordered model. The only abrupt feature exhibited by the current inside the gap occurs in the tunnel regime. The resonant tunneling through the zero-energy bound states leads to a zero-bias anomaly and the subsequent negative differential conductance. As is well known, the position and the height of the peak in the conductance depends on intrinsic width of zero-energy states.<sup>49-52</sup> It is known that the elastic scattering with bulk impurities<sup>53</sup> or a diffusive surface layer<sup>54</sup> provide an intrinsic broadening, which for the case of Born scatterers is  $\propto \sqrt{\Gamma\Delta}$ , where  $\Gamma = 1/2\tau$  is the effective pair breaking parameter locally at the surface. In Fig. 3 we have introduced a small phenomenological broadening of  $10^{-2}\Delta$  to mimic this intrinsic effect.

Let us now consider the case of a momentum conserving contact, which is the usual assumption in the Zaitsev boundary conditions. To gain some insight into the final result, in Fig. 4 we show the contribution of an individual trajectory  $\hat{\mathbf{p}}_F$ . The current and voltage are normalized in units of the gap seen by this trajectory. As can be observed, the current exhibits a pronounced subgap structure at voltages  $eV = \Delta_p/n$ , where  $n$  is an integer number, together with the appearance of negative differential conductance (this can be seen better in the lower panel of this figure). These features are a simple consequence of the resonant tunneling across the zero-energy bound states. Indeed, this type of  $I$ - $V$  has

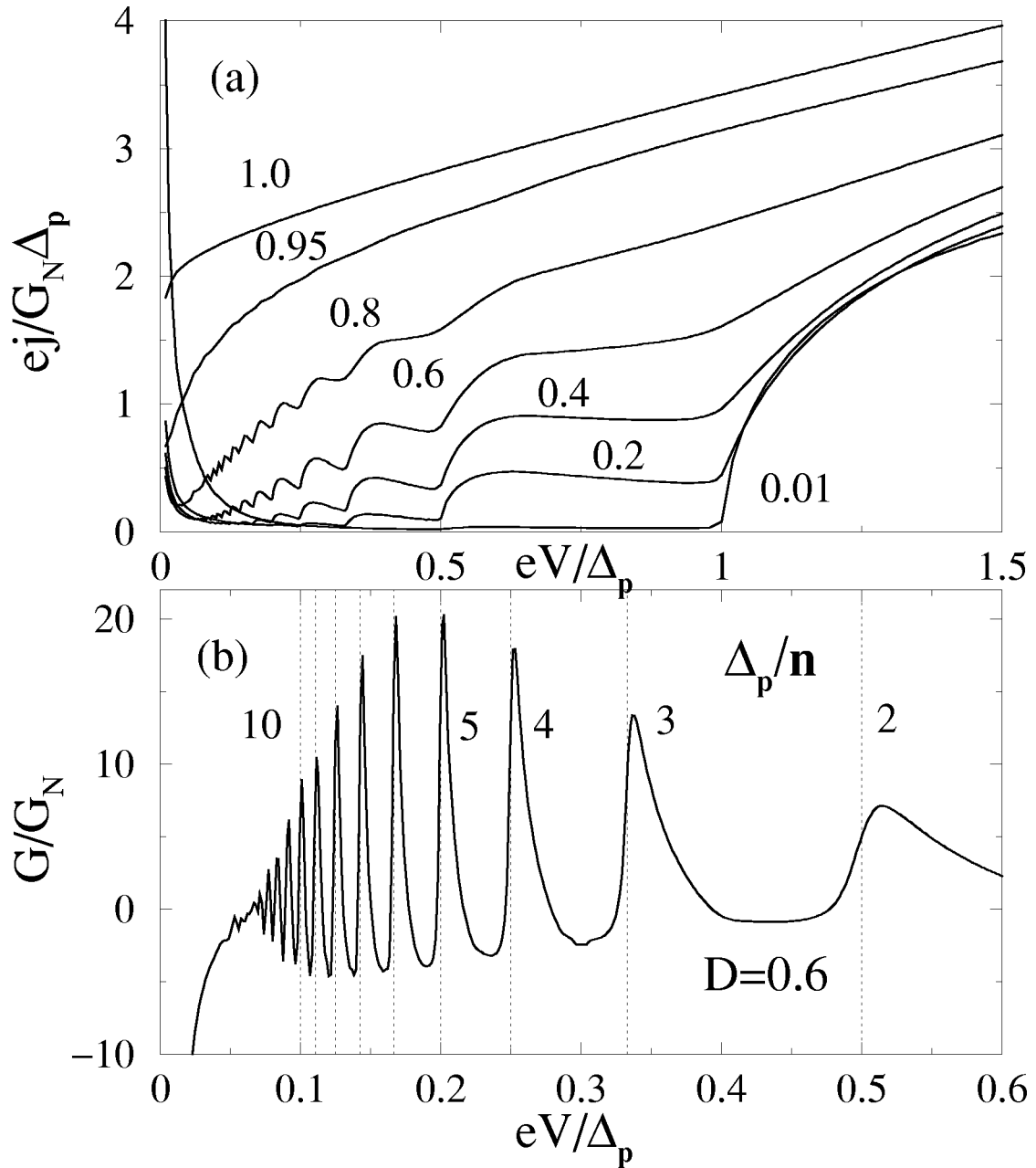


FIG. 4. (a) Trajectory resolved zero-temperature  $I$ - $V$  curves for the  $d$ -wave contact with a momentum conserving interface. The different curves correspond to different values of normal transmission coefficient. In order to see these curves in the same scale the current is normalized by the normal-state conductance  $G_N$  which includes the transmission coefficient. Moreover, the current and the voltage are normalized in units of the momentum-dependent gap. (b) Differential conductance for a transmission  $\mathcal{D}=0.6$ . The vertical lines indicate the positions  $eV_n = \Delta_p/n$ ,  $n=2, \dots, 10$  as a guide for the eye.

been previously obtained in the context of a junction between two conventional superconductors coupled by means of a resonant transmission (see Refs. 55 and 56). Notice also the presence of a zero-bias peak, specially clear for low transparencies, and which is a consequence of the small broadening introduced in the calculation. The total current is obtained by averaging over the different trajectories. Thus the final result depends on the model for the angular dependence of the normal transmission coefficient. With any reasonable model most of the features of the trajectory resolved current disappear. In particular, the subharmonic gap struc-

ture is washed out, and it only remains a peak in the conductance at  $eV \approx \Delta$ .<sup>49</sup>

### V. CURRENT FLUCTUATIONS

During the last years it has become progressively clearer that a deep understanding of the electronic transport in mesoscopic systems requires the analysis of quantities which goes beyond the straightforward measurement of the current-voltage characteristics. In this sense the noise or time-dependent current fluctuations has emerged as a very useful

tool which provides new information on the time correlations of the current, information about channel distributions, statistics, and charge of the carriers.<sup>57</sup> In the case of superconducting contacts, most of the activity has been restricted to the case of *s*-wave superconductors.<sup>58–61</sup> In the case of unconventional superconductors there are only a few theoretical works in the context of hybrid structures like normal-metal/*d*-wave superconductors.<sup>62,63</sup> We believe that in the near future the measurement of current fluctuations will be an important tool for a deeper understanding of the symmetry of the order parameter and origin of the superconductivity in general in the case of high-temperature superconducting materials. For this reason in this section we describe the calculation of the noise spectrum within our approach.

The noise is characterized by its spectral density or power spectrum  $S(\omega)$ , which is simply the Fourier transform at frequency  $\omega$  of the current-current correlation function,

$$\begin{aligned} S(\omega) &= \int d(t'-t) e^{i\omega(t'-t)} \langle \delta_j(t') \delta_j(t) + \delta_j(t) \delta_j(t') \rangle \\ &\equiv \int d(t'-t) e^{i\omega(t'-t)} K(t, t'), \end{aligned} \quad (45)$$

where  $\delta_j(t) = \hat{J}(t) - \langle \hat{J}(t) \rangle$  are the fluctuations in the current. In order to obtain the expression of the current-current correlator, we need an expression for the current operator. Within our model this operator evaluated at the interface can be written as follows:

$$\hat{J}(t) = ie \sum_{\sigma} \{ v_{LR, \sigma} \hat{c}_{L, \sigma}^{\dagger}(t) \hat{c}_{R, \sigma}(t) - v_{RL, \sigma} \hat{c}_{R, \sigma}^{\dagger}(t) \hat{c}_{L, \sigma}(t) \}. \quad (46)$$

This expression is a simple consequence of the continuity equation for the current.<sup>33</sup>

In order to calculate the noise we need in principle to evaluate correlators of four field operators. However, we are working in the framework of a mean-field theory, which means that we can decouple these correlators in terms of one-particle Green's functions using Wick's theorem. With this in mind, it is straightforward to show that the kernel  $K(t, t')$  can be expressed in terms of the interface Keldysh Green's functions as follows:

$$\begin{aligned} K(t, t') &= e^2 \{ \text{Tr} [ \hat{v}_{RL} \hat{G}_{LL}^{<}(t, t') \hat{v}_{LR} \hat{G}_{RR}^{>}(t', t) \\ &\quad + \hat{v}_{LR} \hat{G}_{RR}^{<}(t, t') \hat{v}_{RL} \hat{G}_{LL}^{>}(t', t) \\ &\quad - \hat{v}_{RL} \hat{G}_{LR}^{<}(t, t') \hat{v}_{RL} \hat{G}_{LR}^{>}(t', t) \\ &\quad - \hat{v}_{LR} \hat{G}_{RL}^{<}(t, t') \hat{v}_{LR} \hat{G}_{RL}^{>}(t', t) ] \\ &\quad + (t \rightarrow t') \}, \end{aligned} \quad (47)$$

where the functions  $\hat{G}^{<}$  and  $\hat{G}^{>}$  are related to the usual advanced, retarded, and Keldysh functions in the following way:

$$\begin{aligned} \hat{G}^{<} &= (\hat{G}^K - \hat{G}^R + \hat{G}^A)/2, \\ \hat{G}^{>} &= (\hat{G}^K + \hat{G}^R - \hat{G}^A)/2. \end{aligned} \quad (48)$$

In order to compactify the notation, we introduce the trace  $Tr$  and the matrix  $\tilde{\tau}_3$  which act in the ‘‘reservoir’’ space. Then, the noise kernel reads

$$\begin{aligned} K(t, t') &= -e^2 \text{Tr} [ \tilde{v} \tilde{G}^{<}(t, t') \tilde{\tau}_3 \tilde{v} \tilde{G}^{>}(t', t) \\ &\quad + \tilde{v} \tilde{G}^{>}(t, t') \tilde{\tau}_3 \tilde{v} \tilde{G}^{<}(t', t) ]. \end{aligned} \quad (49)$$

Now, in order to eliminate the Green's functions in favor of the  $T$ -matrix elements, we use the relation

$$\tilde{G}^{<,>} = (\tilde{I} + \tilde{G}^R \circ \tilde{v}) \circ \tilde{G}_{\infty}^{<,>} \circ (\tilde{I} + \tilde{v} \circ \tilde{G}^A), \quad (50)$$

where  $\tilde{G}_{\infty}^{<}(\epsilon) = [\tilde{G}_{\infty}^A(\epsilon) - \tilde{G}_{\infty}^R(\epsilon)] f_{FD}(\epsilon)$  and  $\tilde{G}_{\infty}^{>}(\epsilon) = [\tilde{G}_{\infty}^A(\epsilon) - \tilde{G}_{\infty}^R(\epsilon)] (f_{FD}(\epsilon) - 1)$ . Making use of Eqs. (3)–(7) it is easy to show that the following relation holds:

$$\tilde{v} \circ \tilde{G}^{<,>} = \tilde{T}^R \circ \tilde{G}_{\infty}^{<,>} \circ (\tilde{I} + \tilde{T}^A \circ \tilde{G}_{\infty}^A). \quad (51)$$

This expression allows us to write the noise kernel as follows:

$$\begin{aligned} K(t, t') &= -e^2 \text{Tr} [ [ \tilde{T}^R \circ \tilde{G}_{\infty}^{<} \circ (\tilde{I} + \tilde{T}^A \circ \tilde{G}_{\infty}^A) ] (t, t') \tilde{\tau}_3 \\ &\quad \times [ \tilde{T}^R \circ \tilde{G}_{\infty}^{>} \circ (\tilde{I} + \tilde{T}^A \circ \tilde{G}_{\infty}^A) ] (t', t) + (t \rightarrow t') \}. \end{aligned} \quad (52)$$

As explained in Sec. II, once we have eliminated the full Green's functions in the noise kernel, we can perform the quasiclassical  $\xi$  integration and then replace the Green's functions and  $T$  matrix by their quasiclassical limits. Thus the noise kernel can be finally expressed as

$$\begin{aligned} K(t, t') &= -e^2 \text{Tr} [ [ \tilde{t}^R \otimes \tilde{g}_{\infty}^{<} \otimes (\tilde{I} + \tilde{t}^A \otimes \tilde{g}_{\infty}^A) ] (t, t') \tilde{\tau}_3 \\ &\quad \times [ \tilde{t}^R \otimes \tilde{g}_{\infty}^{>} \otimes (\tilde{I} + \tilde{t}^A \otimes \tilde{g}_{\infty}^A) ] (t', t) + (t \rightarrow t') \}. \end{aligned} \quad (53)$$

Let us stick with the case of a constant bias voltage applied across the interface. In this case, for both contact models considered in Sec. III, we can resolve the current fluctuations in trajectories as follows:

$$S(\omega, t) = e^2 N_F \langle S(\hat{\mathbf{p}}_F, \omega, t) \rangle_{\hat{\mathbf{p}}_F}, \quad (54)$$

where the time-dependent contribution of given trajectory with momentum  $\hat{\mathbf{p}}_F$  can be written as

$$S(\hat{\mathbf{p}}_F, \omega, t) = \sum_{m=-\infty}^{\infty} S_m(\hat{\mathbf{p}}_F, \omega) e^{im\phi(t)}, \quad (55)$$

where the different ac components of the noise can be expressed in terms of the Fourier component of the  $\hat{t}$ -matrix elements in the following way:

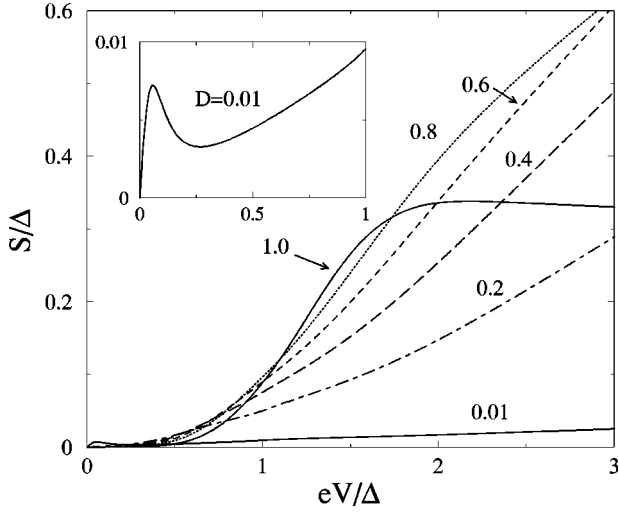


FIG. 5. Zero-frequency shot noise for the disordered contact considered in Fig. 3. The inset shows the low bias limit of the curve in the tunneling regime ( $D=0.01$ ).

$$\begin{aligned}
 S_m(\hat{p}_F, \omega) = & - \int d\epsilon \sum_{n,k,l} \overline{\text{Tr}}\{\tilde{\tau}_{0n}^R(\epsilon) \tilde{g}_n^<(\epsilon) \\
 & \times [\tilde{\Gamma} \delta_{nk} + \tilde{t}_{nk}^A(\epsilon) \tilde{g}_k^A(\epsilon)] \tilde{\tau}_{3k,l}^R(\epsilon + \omega) \tilde{g}_l^>(\epsilon + \omega) \\
 & \times [\tilde{\Gamma} \delta_{lm} + \tilde{t}_{lm}^A(\epsilon + \omega) \tilde{g}_m^A(\epsilon + \omega)] + (\epsilon \leftrightarrow \epsilon + \omega)\},
 \end{aligned} \quad (56)$$

where again we have dropped the subindex  $\infty$  in the surface Green's functions. Notice that in the case of a junction between two superconductors, the noise, as the current, oscillates in time with all the harmonics of the Josephson frequency. Notice also that we have reduced the calculation of this quantity to the determination of the different Fourier components of the  $\tilde{t}$ -matrix elements, which has been detailed in Sec. IV.

In order to illustrate the calculation of the current fluctuations, we consider the contact between  $d$ -wave superconductors analyzed in the previous section. In particular, we present results for the zero-frequency noise at zero temperature  $S$ , i.e., the zero-frequency shot noise. At this point, it is worth remarking that by zero-frequency noise we mean noise at a frequency lower than any relevant energy scale in our problem, gap for instance, and high enough to neglect  $1/f$  noise.<sup>65</sup> Again, the final result depends on the type of contact model under investigation. Let us start discussing the shot noise for the disordered contact. In this case, due to the vanishing of the anomalous Green's functions, the whole calculation reduces to the determination of the quasiparticle contribution, which in terms of the transmission coefficient of Eq. (44) can be written as

$$S = e^2 N_F \int_0^{eV} d\epsilon \mathcal{T}(\epsilon, V) [1 - \mathcal{T}(\epsilon, V)]. \quad (57)$$

This is simply the result that one obtains for a normal contact with an energy and voltage dependent transmission coefficient.<sup>57</sup> In Fig. 5 we show the result of Eq. (57) for

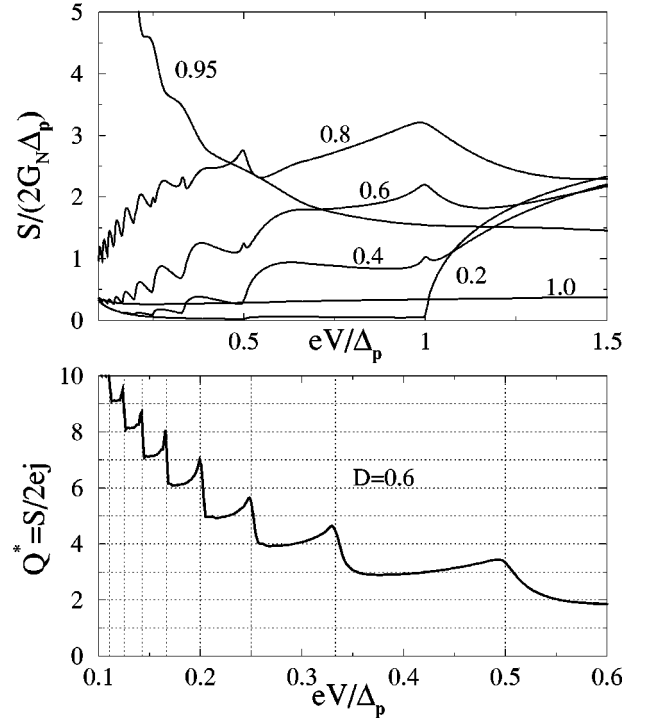


FIG. 6. The upper panel shows the trajectory resolved zero-frequency shot noise for the momentum conserving case considered in Fig. 4. The shot noise and voltage are normalized by the trajectory-dependent gap  $\Delta_p$ . In the lower panel one can see the effective charge defined as  $Q^* = S/2ej$  as a function of voltage for a transmission  $D=0.6$ . The vertical lines indicate the position of the voltages  $eV_n = \Delta_p/n$ ,  $n=2, \dots, 10$ .

different normal transmissions. In the tunneling regime the shot noise is  $S(V) \approx 2ej(V)$  and the most remarkable feature is the zero-bias anomaly (see inset of Fig. 5). In the case of perfect transmission there is a nonzero noise due to the fact that the transmission coefficient  $\mathcal{T}(\epsilon, V)$  is less than one in the gap region. For voltages much greater than the maximum gap,  $\mathcal{T}(\epsilon \gg \Delta, D=1.0) \rightarrow 1$ , which makes the noise at  $D=1.0$  saturate in the high voltage regime.

More interesting is the case of the momentum conserving interface. In Fig. 6 we show the contribution of a trajectory of momentum  $\hat{p}_F$ . As in the case of the current, the shot noise exhibits a rich subharmonic gap structure, which persists almost up to perfect transmission. The shape of the different curves can be understood in the same terms as the BCS case (see Ref. 60), with the additional ingredient of the resonant tunneling through the zero energy states. Of course, as in the case of the current, most of these features disappear after performing the angular average.

In the case of conventional superconductors, the shot noise has been proposed as a tool for measuring the multiple charge quanta transferred by the multiple Andreev reflections.<sup>60</sup> Obviously we can pose here the same question in the case of unconventional superconductors. Indeed, a noise experiment has been recently proposed by Auerbach and Altman<sup>64</sup> to discriminate between two possible explanations of the pronounced subharmonic gap structure observed in YBCO edge junctions,<sup>66</sup> namely, usual multiple Andreev

reflections in a  $d$ -wave superconductor and magnon pair creation in the context of the SO(5) theory. In this latter case the observed charge should be  $Q^* = 2ne$ , where  $n = 1, 2, \dots$ , at a voltage  $eV_n = \Delta/n$ . This result has to be compared with  $Q^* = ne$  expected in the traditional view of MAR. In order to contribute to the solution of this puzzle, we show in Fig. 6 (lower panel) the effective charge,  $Q^* = S/2ej$ , for a transmission  $\mathcal{D} = 0.6$ . This result confirms the traditional interpretation that in the MAR process of order  $n$  a charge  $ne$  is transferred. Usually, in order to observe a clear quantization of the charge one should go to the tunneling regime,<sup>60</sup> but in this case this is not necessary due to the resonant tunneling through the zero energy states. Notice again that this is the contribution of a single trajectory and after angle averaging this clear quantization of the charge with voltage disappears. The exhaustive analysis of the shot noise in  $d$ -wave contacts will be presented in a forthcoming publication.

## VI. CONCLUSIONS

We have shown how a Hamiltonian approach and the quasiclassical theory of superconductivity can be combined to give a powerful tool for the analysis of electronic and transport properties of superconducting junctions. In particular, we have demonstrated that a simple Hamiltonian description of an interface can be used to model a great variety of contacts. This Hamiltonian description can be brought into qua-

sical theory via a  $T$ -matrix equation, resulting in a different formulation of boundary conditions. These boundary conditions do not contain any spurious solutions and can be efficiently solved to compute any transport property. The broad applicability of this formulation covers cases ranging from conventional superconductors to unconventional ones, clean systems, and diffusive ones. Moreover, it can be applied to spin active interfaces and it is well suited for the description of time-dependent phenomena like the  $I$ - $V$  characteristics and the noise properties of junctions with arbitrary transmission and bias voltage. We have illustrated this approach with the calculation of Josephson current in a great variety of situations. The calculation of  $I$ - $V$  characteristics and the noise has been exemplified with the analysis of a contact between two  $d$ -wave superconductors. In particular, we have briefly discussed the use of shot noise as a possible tool for measuring the charge of the Andreev reflections in unconventional superconductors.

## ACKNOWLEDGMENTS

We thank A. Levy Yeyati, A. Martín-Rodero, A. Poenicke, and G. Schön for fruitful discussions. J. C. Cuevas acknowledges the European Community (Contract No. HPMF-CT-1999-00165). M. Fogelström thanks the Swedish Natural Science Research Council (NFR) under Contract No. F620-1072/2000 and the DFG project SFB 195 for support.

- 
- <sup>1</sup>E. L. Wolf, *Principles of Electron Tunneling Spectroscopy* (Oxford University Press, New York, 1985).
- <sup>2</sup>A. Barone and G. Paterno, *Physics and Applications of the Josephson Effect* (Wiley, New York, 1982).
- <sup>3</sup>J.A. Sauls, *Adv. Phys.* **43**, 113 (1994).
- <sup>4</sup>G. Goll, C. Bruder, and H.v. Löhneysen, *Phys. Rev. B* **52**, 6801 (1995).
- <sup>5</sup>A. Sumiyama, S. Shibata, Y. Oda, N. Kimura, E. Yamamoto, Y. Haga, and Y. Onuki, *Phys. Rev. Lett.* **81**, 5213 (1998).
- <sup>6</sup>D.J. Van Harlingen, *Rev. Mod. Phys.* **67**, 515 (1995).
- <sup>7</sup>L.H. Greene, M. Covington, M. Aprili, E. Badica, and D.E. Pugel, *Physica B* **284-288**, 159 (2000).
- <sup>8</sup>L. Alff, S. Kleefisch, U. Schoop, M. Zittartz, A. Marx, and R. Gross, *Eur. Phys. J. B* **5**, 423 (1998).
- <sup>9</sup>C.C. Tsuei and J.R. Kirtley, *Rev. Mod. Phys.* **72**, 969 (2000).
- <sup>10</sup>Y. Maeno, H. Hashimoto, K. Yoshida, S. Nishizaki, T. Fujita, J.G. Bednorz, and F. Lichtenberg, *Nature (London)* **372**, 532 (1994).
- <sup>11</sup>R. Jin, Yu. Zadorozhny, Y. Liu, D.G. Schlom, Y. Mori, and Y. Maeno, *Phys. Rev. B* **59**, 4433 (1999).
- <sup>12</sup>F. Laube, G. Goll, H.v. Löhneysen, M. Fogelström, and F. Lichtenberg, *Phys. Rev. Lett.* **84**, 1595 (2000).
- <sup>13</sup>*Mesoscopic Superconductivity*, Proceedings of the NATO-ARW, edited by F. W. J. Hekking, G. Schön, and D. V. Averin (North-Holland, Amsterdam, 1995).
- <sup>14</sup>C. Lambert and R. Raimondi, *J. Phys.: Condens. Matter* **10**, 901 (1998).
- <sup>15</sup>B. Pannetier and H. Courtois, *J. Low Temp. Phys.* **118**, 599 (2000).
- <sup>16</sup>E. Scheer, P. Joyez, D. Esteve, C. Urbina, and M.H. Devoret, *Phys. Rev. Lett.* **78**, 3535 (1997); E. Scheer, N. Agrait, J.C. Cuevas, A. Levy Yeyati, B. Ludoph, A. Martín-Rodero, G. Rubio, J.M. van Ruitenbeek, and C. Urbina, *Nature (London)* **394**, 154 (1998).
- <sup>17</sup>M. Giroud, H. Courtois, K. Hasselbach, D. Mailly, and B. Pannetier, *Phys. Rev. B* **58**, R11 872 (1998).
- <sup>18</sup>V.T. Petrashov, I.A. Sosnin, I. Cox, A. Parsons, and C. Troadec, *Phys. Rev. Lett.* **83**, 3281 (1999).
- <sup>19</sup>C.L. Chien and D.H. Reich, *J. Magn. Magn. Mater.* **200**, 83 (1999).
- <sup>20</sup>R.J. Soulen, Jr., J.M. Byers, M.S. Osofsky, B. Nadgorny, T. Ambrose, S.F. Cheng, P.R. Broussard, C.T. Tanaka, J. Nowak, J.S. Moodera, A. Barry, and J.M.D. Coey, *Science* **282**, 85 (1998).
- <sup>21</sup>S.K. Upadhyay, A. Palanisami, R.N. Louie, and R.A. Buhrman, *Phys. Rev. Lett.* **81**, 3247 (1998).
- <sup>22</sup>V.V. Ryazanov, V.A. Oboznov, A.Yu. Rusanov, A.V. Veretennikov, A.A. Golubov, and J. Aarts, *Phys. Rev. Lett.* **86**, 2427 (2001).
- <sup>23</sup>G. Eilenberger, *Z. Phys.* **214**, 195 (1968); A.I. Larkin and Y.N. Ovchinnikov, *Zh. Eksp. Teor. Fiz.* **55**, 2262 (1968) [*Sov. Phys. JETP* **28**, 1200 (1969)]; G.M. Eliashberg, *ibid.* **61**, 1254 (1971); [*ibid.* **34**, 668 (1972)].
- <sup>24</sup>J.W. Serene and D. Rainer, *Phys. Rep.* **101**, 221 (1983).
- <sup>25</sup>A.V. Zaitsev, *Sov. Phys. JETP* **59**, 1015 (1984).
- <sup>26</sup>A. Millis, D. Rainer, and J.A. Sauls, *Phys. Rev. B* **38**, 4504 (1988).
- <sup>27</sup>M. Eschrig, *Phys. Rev. B* **61**, 9061 (2000).
- <sup>28</sup>A. Shelankov and M. Ozana, *Phys. Rev. B* **61**, 7077 (2000).

- <sup>29</sup>M. Fogelström, Phys. Rev. B **62**, 11 812 (2000).
- <sup>30</sup>Y. Nagato, K. Nagai, and J. Hara, J. Low Temp. Phys. **93**, 33 (1993).
- <sup>31</sup>N. Schopohl and K. Maki, Phys. Rev. B **52**, 490 (1995).
- <sup>32</sup>J. Bardeen, Phys. Rev. Lett. **6**, 57 (1961).
- <sup>33</sup>C. Caroli, R. Combescot, P. Nozieres, and D. Saint-James, J. Phys. C **4**, 916 (1971).
- <sup>34</sup>A. Martín-Rodero, F.J. García-Vidal, and A. Levy Yeyati, Phys. Rev. Lett. **72**, 554 (1994); A. Levy Yeyati, A. Martín-Rodero, and F.J. García-Vidal, Phys. Rev. B **51**, 3743 (1995).
- <sup>35</sup>J.C. Cuevas, A. Martín-Rodero, and A. Levy Yeyati, Phys. Rev. B **54**, 7366 (1996).
- <sup>36</sup>L.J. Buchholtz and D. Rainer, Z. Phys. B **35**, 151 (1979).
- <sup>37</sup>J. Kurkijärvi, D. Rainer, and J.A. Sauls, Can. J. Phys. **65**, 1440 (1987).
- <sup>38</sup>E.V. Thuneberg, J. Kurkijärvi, and D. Rainer, J. Phys. C **14**, 5615 (1981).
- <sup>39</sup>E.V. Thuneberg, J. Kurkijärvi, and D. Rainer, Phys. Rev. B **29**, 3913 (1984).
- <sup>40</sup>A. Furusaki and M. Tsukada, Physica B **165-166**, 967 (1990).
- <sup>41</sup>C.W.J. Beenakker, Phys. Rev. Lett. **67**, 3836 (1991).
- <sup>42</sup>C.R. Hu, Phys. Rev. Lett. **72**, 1526 (1994).
- <sup>43</sup>Yu.S. Barash, H. Burkhardt, and D. Rainer, Phys. Rev. Lett. **77**, 4070 (1996).
- <sup>44</sup>M. Fogelström, D. Rainer, and J.A. Sauls, Phys. Rev. Lett. **79**, 281 (1997).
- <sup>45</sup>Yu.S. Barash, Phys. Rev. B **61**, 678 (2000).
- <sup>46</sup>L.J. Buchholtz, M. Palumbo, D. Rainer, and J.A. Sauls, J. Low Temp. Phys. **101**, 1079 (1995); **101**, 1099 (1995).
- <sup>47</sup>R.A. Riedel and P.F. Bagwell, Phys. Rev. B **57**, 6084 (1998).
- <sup>48</sup>T. Tokuyasu, J.A. Sauls, and D. Rainer, Phys. Rev. B **38**, 8823 (1988).
- <sup>49</sup>M. Hurd, Phys. Rev. B **55**, R11 993 (1997).
- <sup>50</sup>Yu.S. Barash and A.A. Svidzinsky, Zh. Éksp. Teor. Fiz. **111**, 1120 (1997) [JETP **84**, 619 (1997)].
- <sup>51</sup>M.P. Samanta and S. Datta, Phys. Rev. B **57**, 10 972 (1998).
- <sup>52</sup>T. Löfwander, G. Johansson, and G. Wendin, J. Low Temp. Phys. **117**, 543 (1999).
- <sup>53</sup>A. Poenicke, Yu.S. Barash, C. Bruder, and V. Istyukov, Phys. Rev. B **59**, 7102 (1999).
- <sup>54</sup>M. Fogelström and J. A. Sauls (unpublished); M. Fogelström, J. A. Sauls, M. Covington, M. Aprili, and L. H. Greene (unpublished).
- <sup>55</sup>A. Levy Yeyati, J.C. Cuevas, A. Lopez-Davalos, and A. Martín-Rodero, Phys. Rev. B **55**, R6137 (1997).
- <sup>56</sup>G. Johansson, E.N. Bratus, V.S. Shumeiko, and G. Wendin, Phys. Rev. B **60**, 1382 (1999).
- <sup>57</sup>For a recent review, see Y. Blanter and M. Büttiker, Phys. Rep. **336**, 1 (2000).
- <sup>58</sup>D.V. Averin and H.T. Imam, Phys. Rev. Lett. **76**, 3814 (1996).
- <sup>59</sup>P. Dieleman, H.G. Bukkems, T.M. Klapwijk, M. Schicke, and K.H. Gundlach, Phys. Rev. Lett. **79**, 3486 (1997).
- <sup>60</sup>J.C. Cuevas, A. Martín-Rodero, and A. Levy Yeyati, Phys. Rev. Lett. **82**, 4086 (1999).
- <sup>61</sup>Y. Naveh and D.V. Averin, Phys. Rev. Lett. **82**, 4090 (1999).
- <sup>62</sup>J.X. Zhu and C.S. Ting, Phys. Rev. B **59**, R14 165 (1999).
- <sup>63</sup>Y. Tanaka, T. Asai, N. Yoshida, J. Inoue, and S. Kashiwaya, Phys. Rev. B **61**, R11 902 (2000).
- <sup>64</sup>A. Auerbach and E. Altman, Phys. Rev. Lett. **85**, 3480 (2000).
- <sup>65</sup>D. Koelle, R. Kleiner, F. Ludwig, E. Dantsker, and John Clarke, Rev. Mod. Phys. **71**, 631 (1999).
- <sup>66</sup>O. Neshet and G. Koren, Phys. Rev. B **60**, 9287 (1999).